

# Elbow joint angle and elbow movement velocity estimation using NARX-multiple layer perceptron neural network model with surface EMG time domain parameters

Retheep Raj\* and K.S. Sivanandan

*Department of Electrical Engineering, National Institute of Technology Calicut, India*

## Abstract.

**BACKGROUND:** Estimation of elbow dynamics has been the object of numerous investigations.

**OBJECTIVE:** In this work a solution is proposed for estimating elbow movement velocity and elbow joint angle from Surface Electromyography (SEMG) signals.

**METHODS:** Here the Surface Electromyography signals are acquired from the biceps brachii muscle of human hand. Two time-domain parameters, Integrated EMG (IEMG) and Zero Crossing (ZC), are extracted from the Surface Electromyography signal. The relationship between the time domain parameters, IEMG and ZC with elbow angular displacement and elbow angular velocity during extension and flexion of the elbow are studied. A multiple input-multiple output model is derived for identifying the kinematics of elbow. A Nonlinear Auto Regressive with eXogenous inputs (NARX) structure based multiple layer perceptron neural network (MLPNN) model is proposed for the estimation of elbow joint angle and elbow angular velocity. The proposed NARX MLPNN model is trained using Levenberg-marquardt based algorithm.

**RESULTS:** The proposed model is estimating the elbow joint angle and elbow movement angular velocity with appreciable accuracy. The model is validated using regression coefficient value (R). The average regression coefficient value (R) obtained for elbow angular displacement prediction is 0.9641 and for the elbow angular velocity prediction is 0.9347.

**CONCLUSION:** The Nonlinear Auto Regressive with eXogenous inputs (NARX) structure based multiple layer perceptron neural networks (MLPNN) model can be used for the estimation of angular displacement and movement angular velocity of the elbow with good accuracy.

**Keywords:** Surface electromyography, time domain features, NARX model, Levenberg-marquardt algorithm, neural network, elbow joint angular displacement, elbow angular velocity, integrated EMG, zero crossing

## 1. Introduction

Electrical signals produced by the muscle fibres during activation of muscles are referred to as Electromyography (EMG) signals. Motor units are considered as the basic functional unit of muscle fibre. All type of

skeletal muscle activation begins with the stimulus signal from the central nervous system. This stimulus leads to the generation of action potentials in the motor units of muscle fibres which in turn leads to muscle contraction [1]. Over the last several years, EMG analysis has been used intensively for diagnosing neuromuscular diseases and other clinical analysis [2], fatigue analysis [3] and also for myoelectric control applications [4]. EMG is recorded using both non-invasive techniques, using surface electrodes and invasive technique, using needle electrodes. EMG sig-

---

\*Corresponding author: Retheep Raj, Department of Electrical Engineering, National Institute of Technology Calicut, India. Tel.: +91 9496452144; E-mail: retheepraj@gmail.com.

nal obtained from the surface of the skin above the skeletal muscle is referred as surface electromyography (SEMG). Non-invasive, safe and easiness in measurements made SEMG measurement more popular among researchers even though it is susceptible to problems like crosstalk, artefacts and noises [5].

Muscle contraction can be either isometric or isotonic. The contraction of muscles in which the length of the muscle remains constant is referred to as isometric contraction and the one in which the length changes are referred to as isotonic contraction [6]. SEMG signals contain rich information about the isometric and isotonic muscle contractions [4]. The extracted information can be used for myoelectric control for assisting the amputees. Several works have been done for obtaining the human intentions from the SEMG signals.

Momen et al. implemented a real-time classification of forearm muscle using time domain features and fuzzy C-means clustering algorithm [7]. Ahmad et al. also achieved the classification of elbow angle into three different positions, start, middle and end using fuzzy logic technique [8]. Shalu et al. made an attempt to classify the speed of movement of the elbow into three different classes using fuzzy classifier [9].

Panagiotis et al. tele-operated a robot arm by estimating the elbow joint angle using SEMG signal from biceps and triceps muscles [10]. They used auto regressive moving average with exogenous output (ARMAX) for the estimation. Panagiotis et al. made an attempt to estimate the joint-angle and the force produced by the subjects during elbow and shoulder movements [11]. Here a Multiple input multiple output (MIMO) black box state space model is used for assessment of force and angle. Arthur et al. showed that the EMG signals obtained from the muscles during dynamic condition depends on the angle of joint, velocity of motion and angular acceleration [12]. Sungyoon et al. estimated the intension of human elbow movement at different velocity of flexion and extension and also with varying load [13]. They established that the joint stiffness of elbow had some relations with the angular velocity of movement during loaded condition. Li et al. used a three-layered perceptron neural network model and trained it using back propagation algorithm for the prediction of elbow joint angle. Root mean square (RMS) value of SEMG signal is used as the input parameter for the estimation [14]. Nor Anija et al. carried out research to develop a neural network model for predicting the joint angle and tip force of human thumb [15]. RMS value and moving average

(MA) value are the features used for the prediction, and the training of neural network is done by Levenberg-marquardt based algorithm. Another attempt was made by Zhao et al. for the classification of motion of thumb index and middle finger using parametric autoregressive model [16]. The model parameters are trained using Levenberg-marquardt algorithm based neural network. Castro et al. recorded SEMG signals from biceps and triceps for different static position of elbow joint angle and by using time domain parameter they classified the elbow angle into angles like full extension, full flexion, midway position, etc. [17]. Here the authors used linear discriminant analysis for classification. Another attempt was made by Jang et al. for the assessment of human shoulder angle [18]. Here a spring damper pendulum model is used for relating the shoulder motion and SEMG signals. RMS value of SEMG signal is used as the parameter for estimating the angle. Aung et al. approximated the upper limb joint angle using SEMG signal [19]. Here a back-propagation neural network (BPNN) model is developed for the estimation of joint angle. Levenberg-marquardt algorithm is used for training the BPNN with RMS value of SEMG signal used as the input parameter to the model. They also implemented a simulation software for simulating the output of the model. Yu implemented a third order polynomial function model for the prediction of elbow joint angle [20]. They extracted the RMS value of surface synergic EMG signal for the estimation. N. A. Shirao et al. forecasted finger joint angles using different neural networks with a different number of hidden layer, different initial weight and different number of neurons in hidden layer and the best network is grouped to form committees for validation [21]. Here RMS value of SEMG from index finger is used as the inputs to the neural network. They also concluded that the SEMG signals have a great dependence on the angle of joints, velocity of movements and also on the direction of movement.

From the literature survey, it is clear that there exists a relationship between SEMG, angular displacement and angular velocity of joint angle of elbow or finger and also very little work have been done in estimating self-paced elbow joint angle [22].

In this work, SEMG signals are measured from the biceps brachii muscles of elbow joint during movement of the elbow and the signals are segmented using disjoint window technique. The window size is taken as 250 millisecond duration. Then two time domain parameters, IEMG and ZC are derived from each windowed segments of SEMG signal. Elbow angular dis-

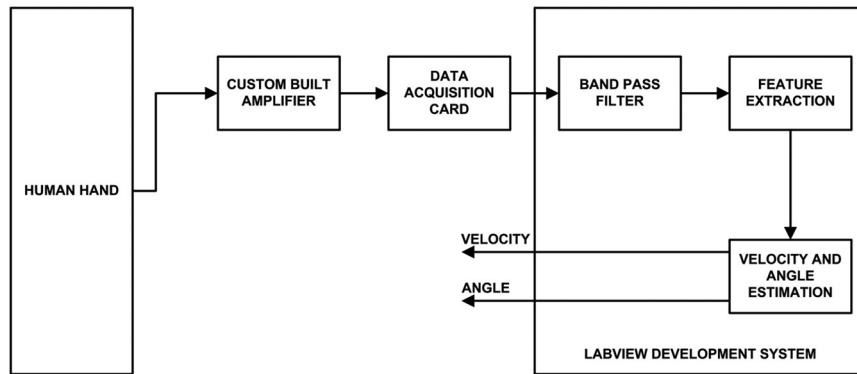


Fig. 1. Block level diagram of experimental setup.

placement and elbow movement velocity is calculated from these parameters using nonlinear auto regressive with exogenous inputs (NARX) structure. The model is trained using Levenberg-marquardt algorithm. The dependence of the SEMG time domain parameters and elbow movement velocities at different angles of elbow joints are also showed in this work.

The rest of the research paper is organised as follows: Section 2 explains the methodology of experimentation, which includes the data acquisition, experimental protocol and feature extraction. Section 3 explains the experimental results and discussions on results and Section 4 explains the conclusions.

## 2. Methodology

### 2.1. Signal acquisition

A custom built bio-amplifier is used for the acquisition of SEMG signals. The bio-amplifier consists of a high speed operational amplifier (OPA 2132P) and a precision low power instrumentation amplifier (INA128P), Texas Instruments make. The bio-amplifier is designed for a gain of 10 and the minimum common mode rejection ratio of the instrumentation amplifier is 100 dB and with a band width of 200 KHz. The output of the bio-amplifier is acquired using National Instruments, My DAQ data acquisition card at a sampling rate of 10 K samples/sec and with an ADC resolution of 16 bit. For the removal of base line shifting, high frequency noises and power line noise, a band pass filter (BPF) and a notch filter is designed using LABVIEW software. A third order infinite impulse response (IIR) Butterworth BPF filter with lower cut off frequency, 20 Hz and upper cut off frequency, 400 Hz followed by a 50 Hz notch filter [5] is implemented for filtering SEMG signal. The block level diagram of the experimental setup is shown in Fig. 1.

### 2.2. Experimental protocol

Four healthy male subjects are allowed to participate in this experiment with an average age of 28 years, an average height of 1.68 m and with an average weight of 64 Kg. Prior consent is taken from the subject before conducting the experiments. SEMG signals are acquired from biceps brachii muscles of dominant hand of the subjects. Three silver-silver chloride (Ag-AgCl) disc type surface electrodes are used for acquiring the signal. Two electrodes are kept as measurement electrode and the third one as the reference electrode. The positive measurement electrode is placed at the centre of the anterior side of biceps brachii, and the negative electrode is placed adjacent to it between the positive electrode and elbow joint. The positive and negative electrodes are placed as close as possible to each other, which means that the distance between the electrodes is equal to the diameter of the electrode [23]. The diameter of the electrode used in the experimentation is 3 cm [24]. The reference electrode is placed on the wrist of the subject's hand.

The subjects are allowed to take complete rest before undergoing experimentation and told to relax all muscles. Subjects are allowed to stay in standing posture and instructed to perform five repetitive flexion and extension movement of the forearm at different velocity. The movement of the forearm ranged from full extension ( $0^\circ$  elbow angle) to full flexion ( $170^\circ$  elbow angle). The full flexion elbow angle may vary with subjects. The elbow angle is measured using a small powered triple axis analog accelerometer, ADXL 335 module attached to the forearm. The tilt angle data are calculated using LabVIEW software and calibrated using a protractor chart attached on the wall. Average velocity for one set of elbow movement cycle, one extension followed by one flexion is calculated from the obtained

angle data. The subjects are instructed to perform flexion and extension of the forearm at different velocity. For getting the SEMG signal at different separable velocities, a predetermined trajectory is displayed on the monitor of the computer and the subjects are asked to follow that trajectory. Also, the subjects are instructed to make the movement as smooth as possible and to keep the non-dominant hand in normal anatomic position (i.e., with the elbow in fully extended position).

### 2.3. Feature extraction

Raw SEMG signals are stochastic, complex and non-linear in nature and because of its stochastic nature it is not possible to extract the information about the human intention from the raw SEMG signal [25]. But at the same time it is observed that certain features of SEMG signals are repeating with muscle dynamics [8]. Several researchers experimented on the classification of SEMG signal based on time domain features [26], frequency domain features [26,27], and time-frequency domain features [28,29] separately and also using combined feature sets [30].

Features are computed from raw SEMG signals by segmenting the signals into small windows. Windows can be sliding type [31] or disjoint window type [32]. Although sliding type windows provide better results [33] when compared with disjoint window, it is not commonly used because of its high computational cost [34].

Here in this work SEMG signal is segmented into 250 millisecond windows using disjoint windowing technique and two time domain features, integrated EMG (IEMG) and zero crossing (ZC) are extracted from the windowed SEMG signal for different velocity of elbow movement.

For a given time series signal, IEMG is the mathematical integral of absolute value of SEMG signal. In other words, it is also defined as the area under the absolute value of windowed SEMG signal. This feature gives the best measure of muscular effect. The equation for calculating IEMG is given by

$$\text{IEMG} = \sum_{k=1}^N |x_k| \quad (1)$$

Where  $x_k$  is the signal and  $N$  is the length of the window.

Zero crossing (ZC) is the measure of number times the SEMG signal amplitude crosses zero line. Sometimes instead of taking crossing zero line as the refer-

ence, a threshold value is kept to avoid the error due to noises and fluctuation in voltage. The formula for ZC is given as

$$\text{ZC} = \sum_{k=1}^N \text{sign}(x_k * x_{k+1}) \text{ and } |x_k * x_{k+1}| \geq \text{threshold value} \quad (2)$$

Where  $x_k$  is the signal and  $N$  is the length of the window. Here the threshold value is taken as 0.1 millivolts [26].

### 2.4. Prediction of elbow velocity and elbow joint angle using NARX modelling

A nonlinear system identification method is used for the prediction of angular velocity and angular displacement of the elbow. A black box type parametric system estimation method is proposed for the estimation. Different types of model structures are available for system identification. One of the major hurdles in the process of system identification is the selection of an apt model for the system under study [35]. For capturing the nonlinear dynamics of a system, NARX structure-based modelling is recommended strongly [34].

Here in this work, a MIMO based NARX structure is used for identification with IEMG and ZC as the input parameters to the structure and velocity of elbow and elbow angular displacement as the outputs. The mathematical equation of NARX model is given by

$$y(t) = f(w(t)) \quad (3)$$

and

$$w(t) = \begin{bmatrix} u(t) \\ u(t-1) \\ \vdots \\ u(t-n_u) \\ y(t-1) \\ y(t-2) \\ \vdots \\ y(t-n_y) \end{bmatrix} \quad (4)$$

Where  $y(t)$  is the predicted output,  $w(t)$  is the regression vector, and  $u(t)$  is the input to the model at time,  $t$ .  $n_u$  and  $n_y$  are the input and output order of the system [36]. The block level diagram of NARX model is shown in Fig. 2. Here in this work, the input and output order value is taken as 3.

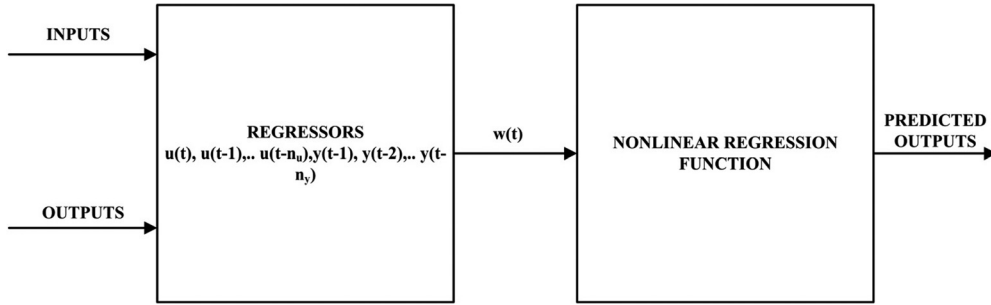


Fig. 2. Block level diagram of NARX model.

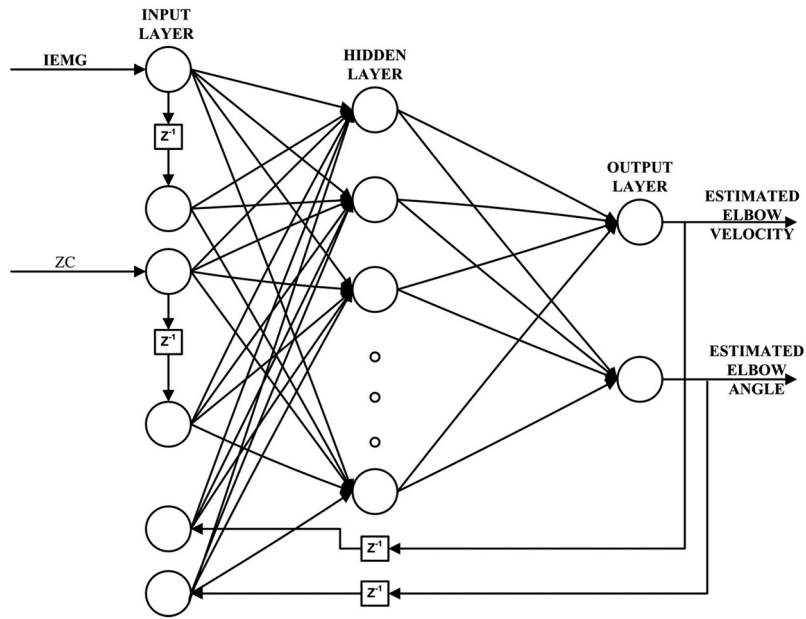


Fig. 3. Structure of the NARX MLPNN model.

The approximation of the function,  $f$  can be carried out by different methods like the neural network, fuzzy logic or neuro-fuzzy methods. Here a neural network based Levenberg-marquardt algorithm (LM) is used for the estimation of the model. The ZC and IEMG data extracted from the SEMG signals are separated randomly into data for training and validation, 70% of the data are used for training and 30% used validating the model.

Levenberg-marquardt algorithm is an improved version of Newton's method. It is an integration of Gauss-newton algorithm and steepest descent algorithm. LM algorithm combines the advantages of both Gauss-newton and steepest descent algorithm, i.e., the speed of convergence of Gauss-Newton method and the stability of Steepest descent method. The structure of the NARX neural network model is given in Fig. 3. For

simplifying the figure the value of  $n_u$  and  $n_y$  are taken as 1. Here the network consists of three layers. First is input layer consists of 12 nodes. Second is hidden layer developed using ten nodes. The third layer is output layer that produces the estimated velocity and joint angle of the elbow. The weight updating equation of LM algorithm is given by

$$w_{n+1} - w_n = - [J^T(x)J(x) + \mu I]^{-1} J^T(x)e(x) \quad (5)$$

Where  $J$  is jacobian matrix,  $e(x)$  is training error,  $I$  is identity matrix. Depending on the value of  $\mu$ , LM algorithm switches between Gauss-newton and steepest descent method. If the value  $\mu$  is very large, then steepest decent algorithm gets executed, and when the value of  $\mu$  is very low, then Gauss-newton method gets executed.



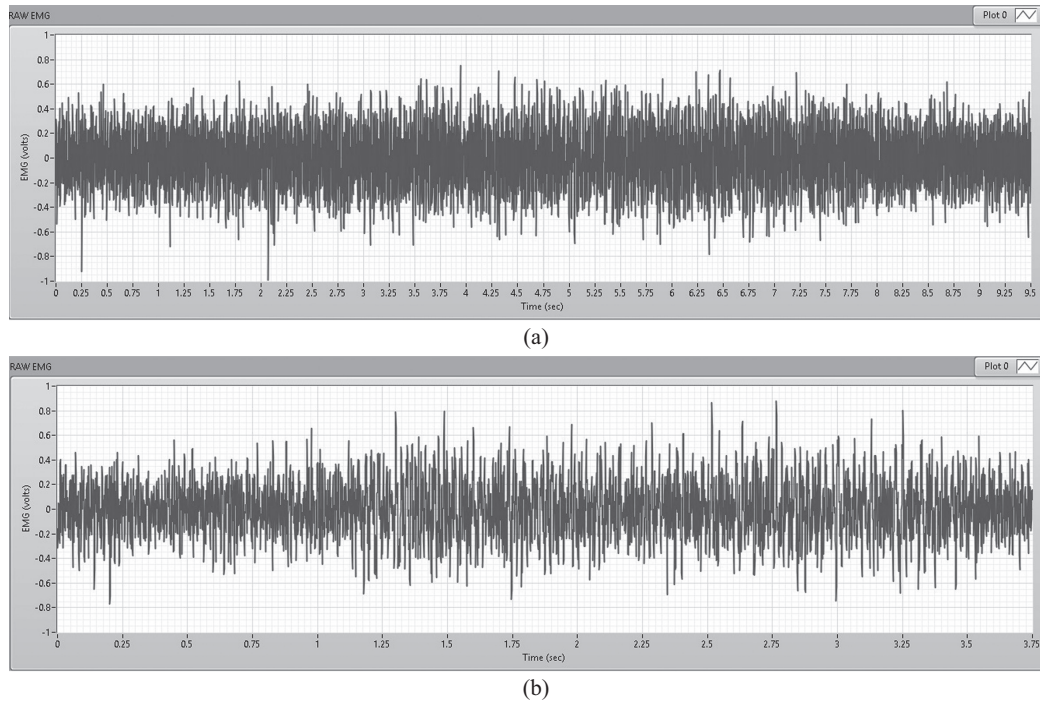


Fig. 4. Representative raw SEMG signals for two different angular velocities with an elbow extension followed by an elbow flexion (a) angular velocity = 32.65 degrees/sec (b) angular velocity = 80 degrees/sec.

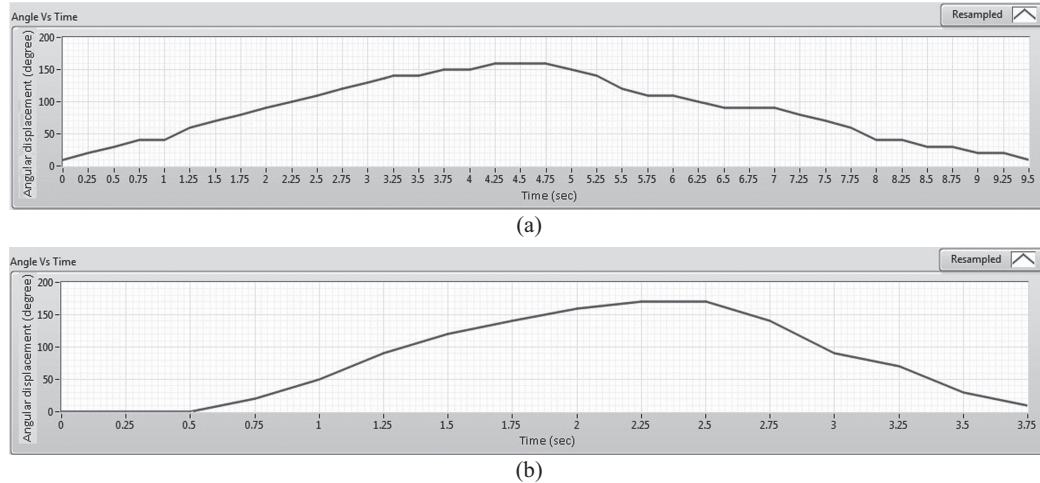


Fig. 5. Representative actual angular displacement measured at two different angular velocities with an elbow extension followed by an elbow flexion (a) angular velocity = 32.65 degrees/sec (b) angular velocity = 80 degrees/sec.

### 3. Results and discussion

Two specimens of raw SEMG signal obtained from the custom bio-amplifier after band pass filtering using LABVIEW development system at two different angular velocities for one elbow extension followed by one elbow flexion are shown in Fig. 4. Correspond-

ing actual elbow angular displacement, measured using analog accelerometer, ADXL 335 module attached to the forearm is shown in Fig. 5. The average angular velocity for one set of elbow extension and elbow flexion is calculated using angle data. IEMG and ZC for different angular velocities are calculated. Representatives of IEMG and ZC parameters for two dif-

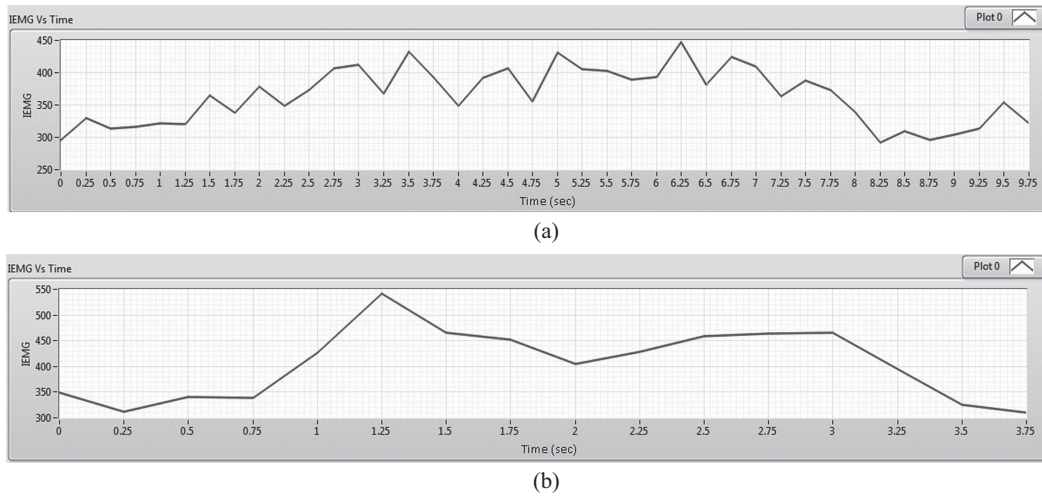


Fig. 6. Representative IEMG at two different angular velocities with an elbow extension followed by an elbow flexion (a) angular velocity = 32.65 degrees/sec (b) angular velocity = 80 degrees/sec.

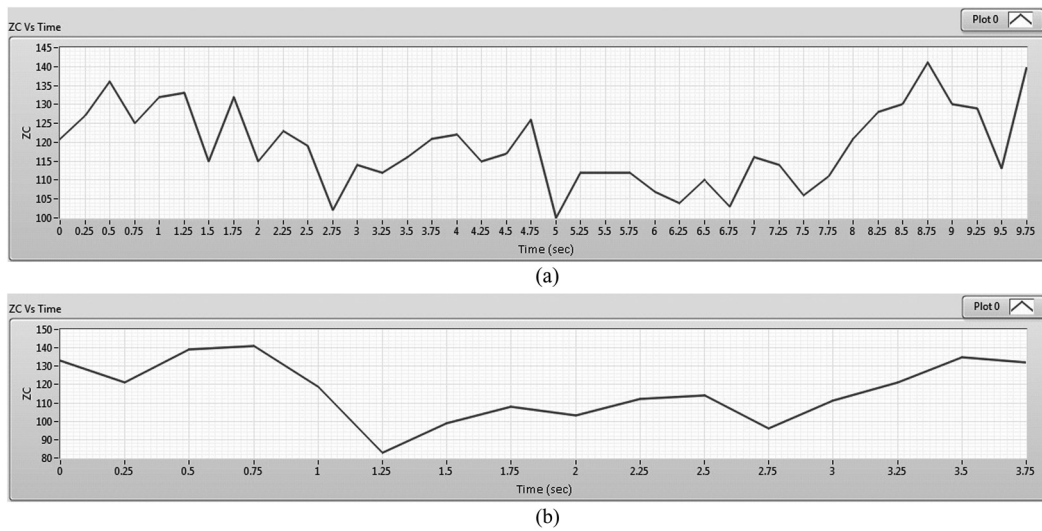


Fig. 7. Representative ZC at two different angular velocities with an elbow extension followed by an elbow flexion (a) angular velocity = 32.65 degrees/sec (b) angular velocity = 80 degrees/sec.

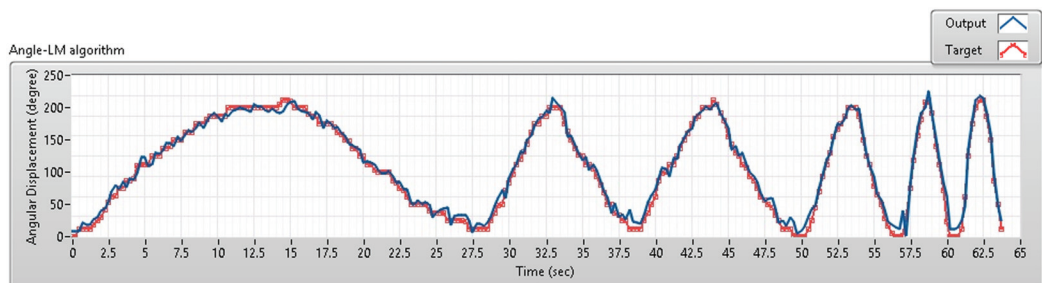


Fig. 8. Graph showing the predicted (output) and estimated (target) value of elbow angular displacement using NARX MLPNN model.

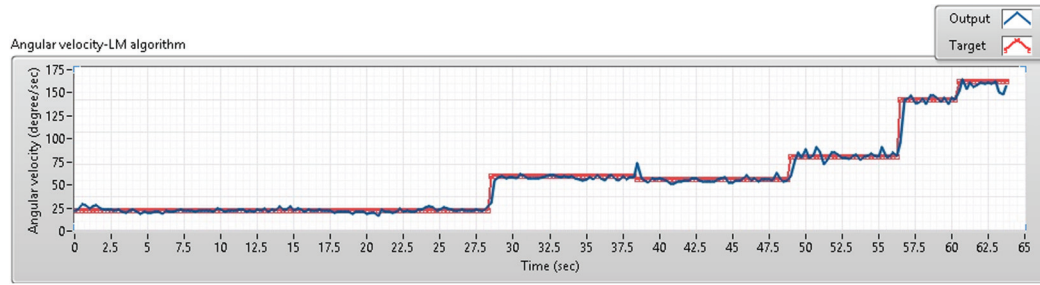


Fig. 9. Graph showing the predicted (output) and estimated (target) value of elbow angular velocity using NARX MLPNN model.

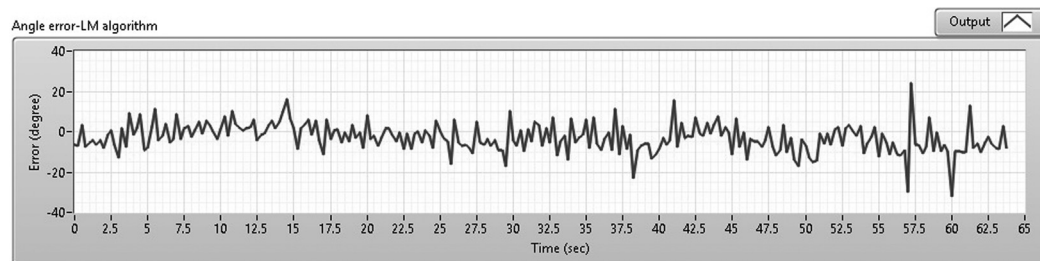


Fig. 10. Graph showing the error between predicted and estimated value of elbow angular displacement using NARX MLPNN model.

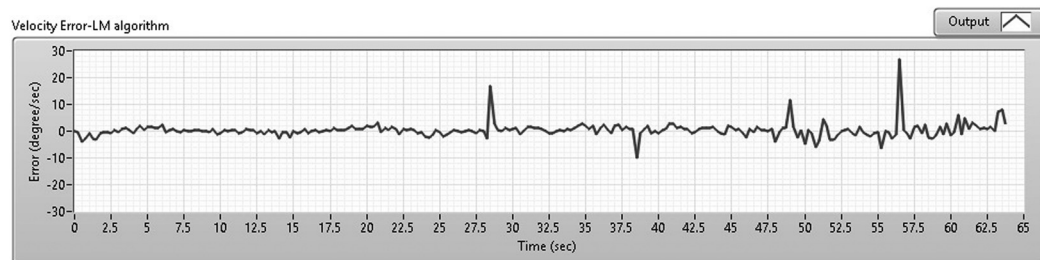
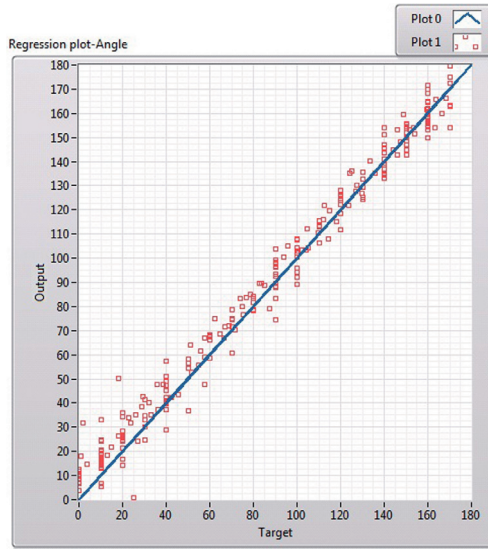


Fig. 11. Graph showing the error between predicted and estimated value of elbow angular velocity using NARX MLPNN model.

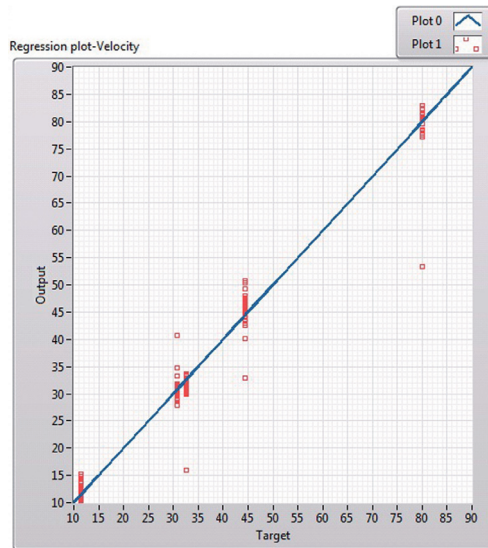
ferent average angular velocities are shown in Figs 6 and 7. It is observed from the Fig. 6 that the value of IEMG is increasing with increase in angular displacement. This increase in IEMG is because of the reason that, as the angular displacement increases, more motor units are recruited and leads to increase in EMG amplitude. IEMG is the mathematical integration of absolute value of EMG, so IEMG also increases. At the same time, the ZC relationship with angular displacement depends on the threshold value selected for calculating ZC. It is observed that the ZC value decreases with increase in angular displacement while the threshold value is zero or close to zero. This decrease in ZC is due to the reason that more motor units are recruited during contraction and so the energy level of EMG increases and then the chances of EMG signal to cross the threshold line decreases. It is clear from the graph that the time domain parameters vary with

the elbow angle position and the elbow movement velocity as indicated in the literature [21]. It is also clear from the graph that the relationship between elbow angular displacement, elbow angular velocity and IEMG is more separable during elbow extension than in elbow flexion. This is because the triceps brachii plays the major role during the elbow flexion rather than biceps brachii. The time domain parameters extracted from SEMG during elbow extensions and flexion are fed as input the NARX MLPNN model trained using Levenberg-marquardt algorithm and the elbow angular velocity and angular displacement were predicted from the obtained model. Figures 8 and 9 indicate the predicted (output) values and actual (target) values of elbow angular velocity and elbow angular displacement during different velocity of elbow extension and flexion.





(a)



(b)

Fig. 12. Regression graph showing the validation of NARX model for (a) elbow angular displacement (2) angular velocity of elbow movement.

The error graph showing the difference between the estimated value and target value for both elbow angular displacement and elbow angular velocity are shown in Figs 10 and 11. The validation of network is done using regression analysis. Figure 12 represents the regression graph, and the value of correlation coefficient (R) is measured. The R-value indicates the deviation between output and the target. The average value of R for angular displacement estimation is 0.9641 and for the estimation of elbow angular displacement, R value is 0.9347. The obtained results are also compared with

Table 1

Regression value of Elbow angular displacement estimation for NARX MLPNN model and ordinary MLPNN model for four different subjects

|           | NARX MLPNN model | Ordinary MLPNN model |
|-----------|------------------|----------------------|
| Subject 1 | 0.9727           | 0.8341               |
| Subject 2 | 0.9713           | 0.8552               |
| Subject 3 | 0.9501           | 0.8125               |
| Subject 4 | 0.9621           | 0.8233               |

Table 2

Regression value of elbow angular velocity estimation for NARX MLPNN model and ordinary MLPNN model for four different subjects

|           | NARX MLPNN model | Ordinary MLPNN model |
|-----------|------------------|----------------------|
| Subject 1 | 0.9492           | 0.6956               |
| Subject 2 | 0.9207           | 0.7021               |
| Subject 3 | 0.9480           | 0.6914               |
| Subject 4 | 0.9209           | 0.6923               |

an ordinary MLPNN model (i.e., with out any delayed signal). The ordinary MLPNN model is nothing but an NARX MLPNN model with  $n_u = n_y = 0$ . Here only the present value of IEMG and ZC are used as the input to MLPNN model for estimation. The mathematical representation of ordinary MLPNN model is given by

$$y(t) = f([iemg(t), zc(t)]) \quad (6)$$

It is observed that the estimation accuracy is better when the proposed NARX MLPNN model is used for estimation. Table 1 indicates the regression coefficient value during the estimation of elbow angular displacement for four different subjects using NARX MLPNN model and ordinary MLPNN model. Table 2 indicates the regression coefficient value during the estimation of elbow angular velocity for four different subjects using NARX MLPNN model and ordinary MLPNN model.

#### 4. Conclusion

In this paper the elbow angular velocity and the elbow joint angular displacement were estimated from the SEMG signals. SEMG signals were acquired from the biceps brachii muscles of the human hand during the elbow movement. The obtained SEMG signals are amplified, filtered and two time domain features (IEMG and ZC) were extracted for different velocity of movement for both flexion and extension of the forearm. The dependence of the extracted time domain parameters on the elbow joint angle and elbow velocity

ties are showed. The obtained time domain parameters are fed to a NARX MLPNN model trained using Levenberg-marquardt algorithm. The obtained result is validated using correlation coefficient, R. The obtained average R value for elbow angular displacement prediction is 0.9641 and obtained average R value for velocity estimation is 0.9347.

## Acknowledgements

The financial support and laboratory facilities provided by the parent institution for conducting this research are gratefully acknowledged. Authors of all the journals listed in the reference section are also acknowledged gratefully. The support and financial assistance provided by TEQIP-II is also acknowledged.

## Conflict of interest

The authors have no conflict of interest to report.

## References

- [1] Yousefi J and Hamilton-Wright A. Characterizing EMG data using machine-learning tools. *Comput Biol Med.* 2014; **51**: 1–13.
- [2] Guler NF and Kocer S. Use of support vector machines and neural network in diagnosis of neuromuscular disorders. *J Med Syst.* 2005; **29**(3): 271–284.
- [3] Venugopal G, Navaneethakrishna M, Ramakrishnan S. Extraction and analysis of multiple time window features associated with muscle fatigue conditions using sEMG signals. *Expert Syst Appl.* 2014; **41**(6): 2652–2659.
- [4] Oskoei MA and Hu H. Myoelectric control systems – A survey. *Biomed Signal Process Control.* 2007; **2**(4): 275–294.
- [5] De Luca CJ, Gilmore LD, Kuznetsov M and Roy SH. Filtering the surface EMG signal: Movement artifact and baseline noise contamination. *J Biomech.* 2010; **43**(8): 1573–1579.
- [6] Jennings D, Flint A, Turton BCH and Nokes LDM. Introduction to medical electronics applications. *Elsevier*; 1995.
- [7] Momen K, Krishnan S, Member S and Chau T. Real-time classification of forearm electromyographic signals corresponding to user-selected intentional movements for multi-function prosthesis control. *IEEE Trans Rehabil Eng.* 2007; **15**(4): 535–542.
- [8] Ahmad SA, Ishak AJ and Ali S. Classification of surface electromyographic signal using fuzzy logic for prosthesis control application. *IEEE Conf Biomed Eng.* 2010; 471–474.
- [9] George S and Sivanandan KS. Speed based EMG classification using fuzzy logic. *Int Rev Comput Softw.* 2012; **7**(3): 950–958.
- [10] Artemiadis PK and Kyriakopoulos KJ. EMG-based teleoperation of a robot arm in planar catching movements using AR-MAX model and trajectory monitoring techniques. *Proc IEEE Int Conf Robot Autom.* 2006; 3244–3249.
- [11] Artemiadis PK and Kyriakopoulos KJ. EMG-based position and force estimates in coupled human-robot systems: Towards EMG-controlled exoskeletons. *Exp Robot Springer.* 2009; 241–250.
- [12] Au ATC and Kirsch RF. EMG-based prediction of shoulder and elbow kinematics in able-bodied and spinal cord injured individuals. *IEEE Trans Rehabil Eng.* 2000; **8**(4): 471–480.
- [13] Lee S, Oh J, Kim Y, Kwon M and Kim J. Estimation of the upper limb lifting movement under varying weight and movement speed. *Int J Eng Ind.* 2011; **2**: 97–105.
- [14] Li D and Zhang Y. Artificial neural network prediction of angle based on surface electromyography. *Int Conf Control Autom Syst Eng.* 2011; 1–3.
- [15] Anija N, Naim S and Ubaidah A. Neuro-based thumb-tip force and joint angle modelling for development of prosthetic thumb control. *Int J Adv Robot Syst.* 2013; **10**: 339.
- [16] Zhao J, Xie Z, Jiang L and Cai H. Levenberg-marquardt based neural network control for a five-fingered prosthetic hand. *IEEE Int Conf Robot Autom Spain.* 2005; 4482–4487.
- [17] Castro MCF, Colombini EL, Aquino PT, Arjunan SP and Kumar DK. sEMG feature evaluation for identification of elbow angle resolution in graded arm movement. *Biomed Eng Online.* 2014; **13**(1): 155.
- [18] Jang G, Kim J, Choi Y and Yim J. Human shoulder motion extraction using EMG signals. *Int J Precis Eng Manuf.* 2014; **15**(10): 2185–2192.
- [19] Paper R, Aung YM and Al-jumaily A. Estimation of upper limb joint angle using surface EMG signal. *Int J Adv Robot Syst.* 2013; **10**: 1–8.
- [20] Yu HJ and Lee AY. Human elbow joint angle estimation using electromyogram signal processing. *IET Signal Process.* 2011; **5**(8): 767–775.
- [21] Shrirao NA, Reddy NP and Kosuri DR. Neural network committees for finger joint angle estimation from surface EMG signals. *Biomed Eng Online.* 2009; **8**: 2.
- [22] Natarajan GS, Winger M, Kim NH and Craelius W. Relating biceps EMG to elbow kinematics during self-paced arm flexions. *Med Eng Phys.* 2012; **34**(5): 617–24.
- [23] Tsai A, Hsieh T, Luh J and Lin T. A comparison of upper-limb motion pattern recognition using EMG signals during dynamic and isometric muscle contractions. *Biomed Signal Process Control.* 2014; **11**: 17–26.
- [24] Venugopal G and Ramakrishnan S. Analysis of progressive changes associated with muscle fatigue in dynamic contraction of biceps brachii muscle using surface EMG signals and bispectrum features. *Biomed Eng Lett.* 2014; **4**(3): 269–276.
- [25] Khushaba RN, Kodagoda S, Takruri M and Dissanayake G. Toward improved control of prosthetic fingers using surface electromyogram (EMG) signals. *Expert Syst Appl.* 2012; **39**(12): 10731–10738.
- [26] Phinyomark A, Phukpattaranont P and Limsakul C. Feature reduction and selection for EMG signal classification. *Expert Syst Appl.* 2012; **39**(8): 7420–7431.
- [27] Phinyomark A, Limsakul C and Phukpattaranont P. A novel feature extraction for robust EMG pattern recognition. *J Comput.* 2009; **1**(1): 71–80.
- [28] Xing K, Yang P, Huang J, Wang Y and Zhu Q. A real-time EMG pattern recognition method for virtual myoelectric hand control. *Neurocomputing.* 2014; **136**: 345–355.
- [29] Englehart K, Hudgins B and Parker PA. Time-frequency based classification of the myoelectric signal: Static. *Proc Annu EMBS Int Conf.* 2000; 7–10.
- [30] Subasi A. Classification of EMG signals using combined features and soft computing techniques. *Appl Soft Comput.* 2012; **12**(8): 2188–2198.

- [31] Tenore FVG, Ramos A, Member S, Fahmy A, Acharya S and Etienne-Cummings R et al., Decoding of individuated finger movements using surface electromyography. *IEEE Trans Biomed Eng.* 2009; **56**(5): 1427–1434.
- [32] Huang Y, Englehart KB, Member S, Hudgins B and Chan ADC. A gaussian mixture model based classification scheme for myoelectric control of powered upper limb prostheses. *IEEE Trans Biomed Eng.* 2005; **52**(11): 1801–1811.
- [33] Englehart K, Hudgins B and Member S. A robust, real-time control scheme for multifunction myoelectric control. *IEEE Trans Biomed Eng.* 2003; **50**(7): 848–854.
- [34] Liu Y. Towards a high-stability EMG recognition system for prosthesis control: A one-class classification based non-target EMG pattern filtering scheme. *IEEE Int Conf Syst Man Cybern.* 2009; 4752–4757.
- [35] Pearson RK. Selecting nonlinear model structures for computer control. *J Process Control.* 2003; **13**(1): 1–26.
- [36] Babuska R and Verbruggen H. Neuro-fuzzy methods for nonlinear system identification. *Annu Rev Control.* 2003; **27**(1): 73–85.